# Adaptive Wavelet Packet Modulation

Marwa Chafii, Jacques Palicot, Rémi Gribonval, Faouzi Bader

# Adaptive Wavelet Packet Modulation

Marwa Chafii, *Member, IEEE*, Jacques Palicot, *Member, IEEE*, Rémi Gribonval, *Fellow, IEEE*, and Faouzi Bader, *Senior, IEEE*

***Abstract*—In this paper, we propose a new adaptive modulation based on the wavelet packet transform, which targets a good resistance against frequency selective channels while avoiding a large PAPR. Classical multi-carrier modulation schemes divide the channel bandwidth into narrowband sub-channels to improve its robustness against frequency selective fading. However, they suffer from the peak-to-average power ratio (PAPR) problem which occurs due to a random constructive addition of sub-carriers. By contrast, single carrier modulation schemes, where each transmitted symbol fully occupies the bandwidth, are more sensitive to frequency selective environments and less affected by the PAPR problem. In this work, we show how the bandwidth division can be reconfigurable and adapted to the channel properties, and we provide several examples to prove that the proposed adaptive modulation represents an alternative modulation which is adjustable between two extreme cases: single carrier modulation and classical multi-carrier modulation.**

***Index Terms*—Multi-Carrier Modulation (MCM), Wavelet transform, Orthogonal Frequency Division Multiplexing (OFDM), Peak-to-Average Power Ratio (PAPR).**

## I. Introduction

**Multi-carrier vs. single-carrier waveforms** Multi-carrier modulation (MCM) schemes represent attractive modulation techniques for data transmission. In particular, orthogonal frequency division multiplexing (OFDM) system, which has been adopted by long term evolution (LTE) standard and its evolutions [1], is widely used in various wireline and wireless applications and standards, mainly due to its ability to cope with frequency selective fading environments [2]. In fact, OFDM divides the allocated bandwidth into several orthogonal narrow sub-bands and performs parallel data multiplexing. The partition of the bandwidth provides a resistance against frequency selective channels, to the extent that if the channel is attenuated at a certain frequency, only the symbol carried upon the associated sub-band will be affected, and not the entire transmitted symbols. However, OFDM, as well as most classical MCM schemes, suffers from large peak-to-average power ratio (PAPR) [3]. The constructive random addition of the sub-carriers generates high power fluctuations which causes non-linear distortions when the MCM signal is introduced into a high power amplifier (HPA). An input back-off is then necessary to amplify the signal in the linear domain of the HPA characteristic, which corresponds to a poor efficiency. The HPA accounts for more than $60\%$ of the power consumption at the transmitter side [4], hence the PAPR problem seriously limits the energy-efficiency of MCM systems.

The obvious solution of the PAPR issue is the single carrier modulation (SCM) schemes, where the signal envelope is not affected by overlapping sub-carriers, but depends only on the employed constellation and the selected roll-off of the Nyquist filter [5]. While this ability of SCM to control the PAPR is notable, SCM schemes are not as robust as MCM schemes against fading environments. When the channel encounters fading around some specific frequencies, all the transmitted symbols will be affected since each symbol occupies the whole bandwidth.

**PAPR/BER trade-off** Splitting the whole bandwidth into narrow sub-bands certainly offers strong resilience in frequency selective fading environments, but limits considerably the PAPR performance. While transmitting each symbol in the full bandwidth, whereas it allows a reduced PAPR, increases the sensitivity towards degraded environments. The target of this paper is to propose a new adaptive waveform to deal with this trade-off, which can be viewed as a PAPR/BER (bit error rate) compromise. The proposed adaptive wavelet packet modulation (AWPM) adapts the bandwidth repartition to the channel characteristics. Depending on the frequency selectivity of the channel, the new proposed waveform can be adjustable between two corner cases: SCM and MCM. The adaptation of the bandwidth subdivision is only possible with a flexible time-frequency tiling. The wavelet packet transform satisfies this property unlike OFDM and the single carrier waveform as discussed in Section II and Section III.

**PAPR reduction techniques** In the literature, several PAPR reduction techniques have been proposed and compared. We mainly identify probabilistic techniques [6], coding techniques [7], and adding signal techniques [8]. One of the most used PAPR reduction techniques that trades the PAPR performance against the BER performance is clipping [9]. This operation consists in clipping the peaks that exceed a predetermined threshold. Since clipping is a non-linear function, it generates distortions that degrade the BER performance. This leads to a PAPR/BER trade-off.

Among PAPR reduction techniques in the literature, some (such as coding techniques) act on the input symbols before modulation. Others act after the modulation such as clipping. The approach in this paper is different: we actually propose a new waveform that generates a signal with low PAPR *by construction*, and without any PAPR reduction processing. Naturally, further PAPR reduction techniques can be applied to AWPM the same way they are applied to OFDM. We show

M. Chafii, J. Palicot and Faouzi Bader are with the CentraleSupélec/IETR, 35576 Cesson-Sévigné, France (e-mail:{marwa.chafii, jacques.palicot,faouzi.bader} @supelec.fr).

R. Gribonval is with Inria Rennes-Bretagne Atlantique, 35042 Rennes Cedex, France (e-mail:remi.gribonval@inria.fr.

This work has received a French state support granted to the CominLabs excellence laboratory (TEPN project) as well as *Enhanced PHY for cellular Low power communication IoT (EPHYL)* project. These projects are managed by the National Research Agency under reference Nb. ANR-10-LABX-07-01 and Nb. ANR-16-CE25-0002-03 respectively. The authors would also like to thank the Region Bretagne, France for its support of this work.

in Section VI-D that the PAPR/BER trade-off achieved by AWPM outperforms the one attained by clipping when applied to OFDM.

**Adaptive transmission techniques** Multiple adaptive techniques have been presented in the literature. Adapting the transmission parameters for OFDM have been proposed by Kalet [10] and developed later by Chow et al. in [11], and Czylwik et al. in [12]. The transmission parameters are adapted to the channel characteristics, in order to improve the system performance in terms of spectral efficiency, transmission rate, and BER. Different adapting parameters have been proposed: the allocated power of each sub-carrier, the constellation scheme, the coding, the intercarrier-spacing, the length of the guard interval among others. To the best of our knowledge, adapting the modulation waveform along with the partition of the bandwidth has never been investigated in the literature, AWPM is a new adaptive scheme that enables selecting the waveform that gives the best PAPR/BER trade-off.

The rest of this paper is organized as follows. In Section II, a classification of multi-carrier modulations based on time-frequency properties of the waveform is exposed, while Section III surveys the wavelet packet modulation, and shows how the wavelet packet transform enables flexible time-frequency tilings, to support its use in the proposed scheme. The principle of the proposed AWPM scheme is described in Section IV. The performance of the AWPM system is assessed and commented in Section V for a specific channel, and in Section VI for a Rayleigh frequency selective channel from LTE standard. Finally, Section VII concludes the paper and opens new perspectives for the proposed modulation scheme.

## II. Time-frequency tilings associated to multi-carrier modulation systems

This section proposes a classification of MCM schemes regarding the time-frequency characteristics of the transmitted signal. The purpose of this section is to show that the wavelet packet transform has the most relevant time-frequency properties to answer the PAPR/BER trade-off goal, compared with other presented schemes. The time-frequency resolution of the transmitted signal depends on the way data is multiplexed and modulated. The time duration and the frequency width of the sub-carriers can be allocated uniformly or non-uniformly for each symbol. The selected multiplexing and modulation methods vary from one application to another, and the representation of the signal in the time-frequency plane changes accordingly. Basically, two typical tilings of the time-frequency plane can be distinguished: regular sharing of the bandwidth which leads to Gabor-based MCM schemes, or non-regular sharing of the bandwidth which yields wavelet-based MCM systems.

### A. Gabor-based MCM schemes

A Gabor family in $L_2(\mathbb{R})$ is a family of functions $(g_{m,n})_{(m,n)\in\mathbb{Z}^2} \in L_2(\mathbb{R})$ that verify:

$$(\forall t \in \mathbb{R}) \quad g_{m,n}(t) \quad = \quad g(t-nT)\mathrm{e}^{j2\pi m\Delta F t},$$

where $g$ is a prototype function or a window, $T$ is the symbol period, and $\Delta F$ is the inter-carrier spacing. The functions $g_{m,n}$ are derived using time translations and frequency modulations of the window $g$.

In order to provide an insight into the time-frequency properties of Gabor basis, Fig. 1 depicts the time-frequency boxes, also known as "Heisenberg rectangles" [13], which reflects the time localization and the frequency localization of a Gabor-based modulated signal, defined as:

$$x(t) \quad = \quad \sum_{n\in\mathbb{Z}} \sum_{m\in M} C_{m,n} g_{m,n}(t), \tag{1}$$

where $M$ is the number of sub-carriers considered, and $C_{m,n}$ are the input symbols associated to an $\mathcal{M}$-ary constellation. In this figure, the time-frequency plane is represented by boxes translated uniformly in time and frequency directions.

Most classical MCM systems can be classified as Gabor-based MCM schemes. This includes notably: OFDM (orthogonal frequency division multiplexing), FBMC (filter bank based multi-carrier) [14], FMT (filtered multitone) [15], NOFDM (non-orthogonal frequency division multiplexing) [16], GFDM (generalized frequency division multiplexing) [17], and UFMC (universal filtered multi-carrier) [18].

It is worth mentioning that according to our previous work in [3]. OFDM has the best PAPR performance among Gabor-based MCM schemes for the same number of sub-carriers.

### B. Wavelet-based MCM schemes

The wavelet transform is based on a family of wavelets and scaling functions defined as contracted and translated versions from a wavelet mother function $\psi$ and a scaling mother function $\phi$ as follows:

$$\psi_{j,k} \quad = \quad 2^{j/2}\psi(2^j t - kT), \tag{2}$$

$$\phi_{j,k} \quad = \quad 2^{j/2}\phi(2^j t - kT). \tag{3}$$

Fig. 2 suggests a time-frequency tiling associated to a wavelet-based MCM signal defined as:

$$\begin{aligned} x(t) \quad = \quad & \sum_{n\in\mathbb{Z}} \sum_{j=J_0}^{J} \sum_{k=0}^{2^j-1} w_{j,k}\psi_{j,k}(t-nT) \\ & + \sum_{n} \sum_{q=0}^{2^{J_0}-1} a_{J_0,q}\phi_{J_0,q}(t-nT), \end{aligned} \tag{4}$$

where $J_0$ ($J$ resp.) is the first (last resp.) scale considered, and $w_{j,k}, a_{J-L,k}$ are the input symbols associated to an $\mathcal{M}$-ary constellation.

Unlike the regular time-frequency tiling of Gabor-based systems, the wavelet transform offers good frequency (poor temporal respectively) localization at low frequencies. The wavelet-based MCM system is known in the literature as Wavelet-OFDM [19], [20] or as orthogonal wavelet division multiplexing (OWDM) [21].

Although the wavelet transform is flexible compared with Gabor transform, it is constrained by a decomposition of a dyadic growth. The wavelet packet transform (WPT), allows more flexible tiling of the time-frequency plane. The wavelet

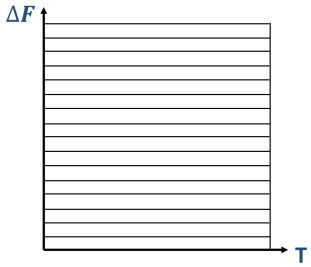


Figure 1: Time-frequency plane associated to Gabor transform.

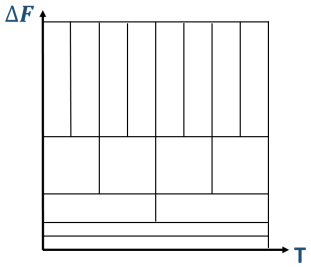


Figure 2: Time-frequency plane associated to the wavelet transform.

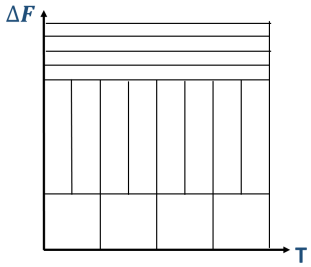


Figure 3: Time-frequency plane associated to the wavelet packet transform.

transform is then a particular case of the WPT. Fig. 3 shows an example of the time-frequency plane related to WPT.

Unlike the other transforms exposed in this section, the flexibility of the WPT provides a better ability to satisfy the required time-frequency properties of the resulting signal in order to achieve the desired PAPR/BER performance. This statement is supported by the analysis and the simulations later in this paper. Since WPT is adopted by the proposed AWPM scheme in this work, a detailed description of its characteristics is provided hereafter.

## III. Wavelet packet modulation

The early work on the wavelet packet modulation (WPM) come back to Lindsey [22], who has investigated the application of the wavelet packet basis in orthogonal data multiplexing in communication systems. WPM or wavelet packet-OFDM [23]–[25], is based on the WPT by modulating the input symbols. Due to the time-frequency properties of this transform, WPM allows more flexibility for signal modulation.

### A. Wavelet packet basis

The wavelet packets have been introduced by Coifman, Meyer and Wickerhauser [26]. The set of wavelet packet orthonormal basis can be represented schematically by a binary tree as shown in Fig. 4. Every node of the tree is identified by the index $(j,\ell)$ where $J-j$ is the depth of the tree, and $m$ is the number of nodes located on the left at the same depth. Each node of the tree is associated to a sub-space $\mathrm{P}_j^m$, which is defined as a direct sum $\oplus$ of its two children nodes:

$$\mathrm{P}_j^\ell = \mathrm{P}_{j-1}^{2\ell} \oplus \mathrm{P}_{j-1}^{2\ell+1}. \tag{5}$$

Each sub-space $\mathrm{P}_j^\ell$ is represented by a wavelet packet orthonormal basis $\{\mathcal{P}_j^\ell(2^{-j}t-k)\}_{k\in\mathbb{Z}}$, which can be derived by applying recursively a high-pass filter $f^h$ and a low-pass filter $f^l$ [1] to the dilated basis functions of the parent node [13]

$$\mathcal{P}_{j-1}^{2\ell}(2^{-j}t) = \sum_k f^l(k)\mathcal{P}_j^\ell(2^{-j}t-k) \tag{6}$$

$$\mathcal{P}_{j-1}^{2\ell+1}(2^{-j}t) = \sum_k f^h(k)\mathcal{P}_j^\ell(2^{-j}t-k). \tag{7}$$

[1]The filters associated to a wavelet and a scaling function are quadrature mirror filters (QMF), and should satisfy other properties that can be found in [27].

The vector space $P_J^0$ denotes the root of the tree. The basis of the root node is expressed as $\{\mathcal{P}_J(2^{-J}t-k)\}_{k\in[\![0,2^J-1]\!]}$. After fixing the filter coefficients and the root node basis, all the bases associated to the rest of the nodes are defined.

### B. Admissible tree

Several admissible trees can be identified from a wavelet packet binary tree (see Fig. 4). A tree is qualified as *admissible* if every node of the tree has 0 or 2 children nodes as in the example plotted in Fig. 5. Along the branches of an admissible tree, the vector spaces associated to sibling nodes are pairwise orthogonal. The union of the associated wavelet packet basis defines an orthogonal basis of the vector space $P_J^0$ associated to the root of the tree.

Note that selecting an admissible tree for data modulation leads to specific time-frequency properties of the resulting signal. The number of possible admissible trees is actually more than $2^{2^{J-1}}$ [13], which reflects the remarkable flexibility of the WPT.

Let $\mathcal{T}$ an admissible tree and $\{g_m^{\mathcal{T}}(t)\}_{m=0}^{2^J-1}$ the associated basis. The signal $x(t)$ of a duration $T$, which results from the modulation of input symbols $\{a_m\}$, is expressed as follows:

$$x(t) = \sum_{n\in\mathbb{Z}}\sum_{m=0}^{2^J-1} a_m g_m^{\mathcal{T}}(t-nT). \tag{8}$$

## IV. Principle of the proposed AWPM scheme

AWPM suggests the adaptation of the bandwidth partition to the environment properties, by exploiting the flexibility of the WPT. In this section, we describe the general assumptions of the AWPM scheme and develop the adaptive algorithm of selecting the "best" bandwidth partition for a defined known channel. Some exchanging scenarios between the transmitter and the receiver are also exposed in this section.

### A. General principle

The objective of the AWPM scheme can be reformulated as finding the best admissible tree subject to the criterion of peak-to-average power ratio/bit error rate (PAPR/BER) trade-off. Dealing with this trade-off means dividing the bandwidth only in the frequencies attenuated by the channel fading to achieve good BER performance, while not doing so when the channel presents good characteristics in order to reach good PAPR performance.

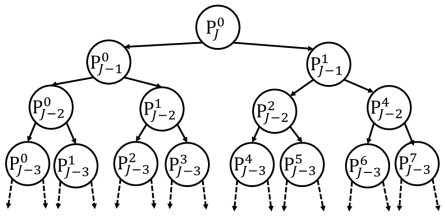

Figure 4: Binary tree associated to wavelet packet basis.

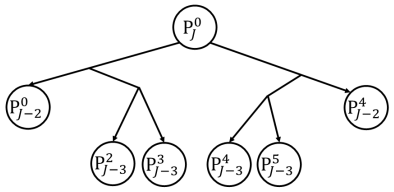

Figure 5: Example of admissible wavelet packet binary tree.

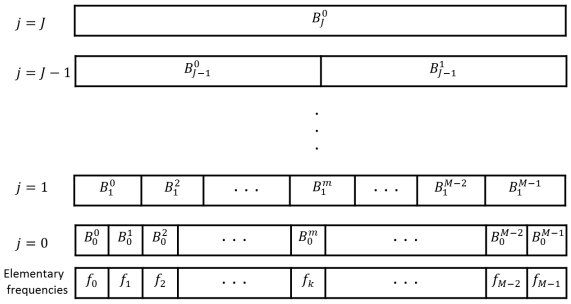


Figure 6: Representation of sub-bands $B_j^m$.

The WPT allows a flexible partition of the frequency axis. The set of possibilities of bandwidth division is represented by the set of all admissible trees associated to all possible wavelet packet bases. For instance, a complete decomposition of the bandwidth (e.g. OFDM case) is reached by selecting the deep nodes (leaves) of the tree. Not dividing the bandwidth consists in selecting the root of the tree (e.g. single carrier case).

### *B. Notations and definitions*

In order to describe the AWPM waveform construction, we provide here the appropriate notations.

*a) Elementary frequency $f_k$:* We assume that the whole spectral bandwidth of transmitted signal can be divided into $M$ elementary sub-bands $\{B_0^m\}_{m\in[\![0,M-1]\!]}$ associated to $M$ elementary frequencies $\{f_k\}_{k\in[\![0,M-1]\!]}$ which are represented by the leaves $\{P_0^m\}_{m\in[\![0,M-1]\!]}$ of the binary wavelet packet tree.

*b) sub-band $B_j^m$ (see Fig. 6):* Every node $\mathrm{P}_\mathrm{j}^\mathrm{m}$ of the wavelet packet tree is assigned to a sub-band $B_j^m$. The sub-band $B_j^m$ is a set of elementary frequencies:

$$f \in B_j^m \quad \Longleftrightarrow \quad f \in \{f_k\}_{k\in[\![m2^j,(m+1)2^j-1]\!]}.$$

*c) How to measure the state of the channel?:* For the purpose of evaluating the communication channel fading, many features can be envisioned. For example, the amplitude $|H|$ of the frequency response of a channel $h$ can be considered. We can state that the lower is the amplitude $|H(f_k)|$, the more affected by the channel fading is the associated frequency $f_k$. Other parameters can be considered such as the power $|H(f)|^2$ or the signal-to-noise ratio (SNR) as a function of the frequency $f$.

In order to estimate how frequency-selective is the channel in a sub-band $B_j^m$, the variation of the channel in this sub-band can be examined. The channel variation can be evaluated by comparing the ratio or the difference between the measures of the state of the channel associated to the elementary frequencies $\{f_k\}$ in the sub-band $B_j^m$.

Hereafter, the channel amplitude in dB $|H(f)|_{\text{dB}} = 20\log_{10}|H(f)|$ is selected as an indicator of the quality of the channel. The difference between the parameters $|H(f_k)|_{\text{dB}}$ for elementary frequencies belonging to a sub-band $B_j^m$ is chosen to be a measure of the frequency selectivity of the channel in this sub-band.

*d) Threshold of attenuations $\alpha$:* Let $\alpha$ be real number in dB. For each elementary frequency $f_k$ is assigned a parameter $\theta^\alpha(f_k) \in \{0,1\}$ defined as follows

$$\theta^\alpha(f_k) \quad = \quad \begin{cases} 1 & \text{if} \quad |H(f_k)|_{\text{dB}} \geq \alpha \\ 0 & \text{elsewhere} \end{cases}. \tag{9}$$

If $\theta^\alpha(f_k) = 1$, we state that the frequency $f_k$ is "non-attenuated" by the channel fading. Otherwise, it is stated "attenuated". It should be recalled that, $|H(f_k)|_{\text{dB}}$ could be replaced in (9) by another channel measure including the $|H(f_k)|$, the $|H(f_k)|^2$, and the SNR$(f_k)$ among others.

We define $\Theta^{\alpha,1}$ as the set of sub-bands $B_j^m$ containing *only* non-attenuated frequencies. Similarly, we define $\Theta^{\alpha,0}$ as the set of the sub-bands $B_j^m$ containing only attenuated frequencies, i.e

$$B_j^m \in \Theta^{\alpha,1} \quad \Longleftrightarrow \quad \forall f_k \in B_j^m \quad \theta^\alpha(f_k) = 1, \tag{10}$$

$$B_j^m \in \Theta^{\alpha,0} \quad \Longleftrightarrow \quad \forall f_k \in B_j^m \quad \theta^\alpha(f_k) = 0. \tag{11}$$

*e) Threshold of variations $\beta_0$:* Let $\beta_0$ be a real number in dB. For each attenuated sub-band $B_j^m \in \Theta^{\alpha,0}$, we assign a parameter $\delta^{\beta_0}(B_j^m) \in \{0,1\}$ defined as follows:

$$\delta^{\beta_0}(B_j^m) = \begin{cases} 1 & \text{if } \max\limits_{f_k\in B_j^m} |H(f_k)|_{\text{dB}} - \min\limits_{f_k\in B_j^m} |H(f_k)|_{\text{dB}} \leq \beta_0 \\ 0 & \text{elsewhere} \end{cases}.$$

When $\delta^{\beta_0}(B_j^m) = 1$, the difference between the frequency responses of the channel does not exceed the threshold $\beta_0$ for each pair of elementary frequencies $f_k$ belonging to the sub-band $B_j^m$. In other words, the channel $h$ does not vary "significantly" regarding to the threshold $\beta_0$ for $B_j^m$.

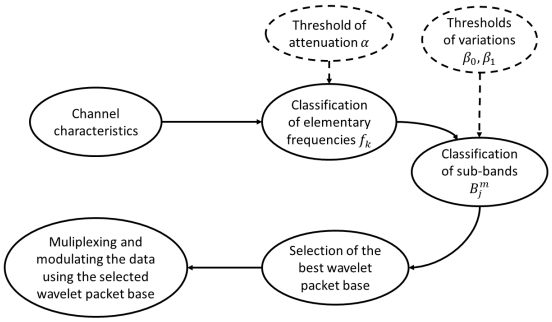


Figure 7: AWPM modulation scheme.

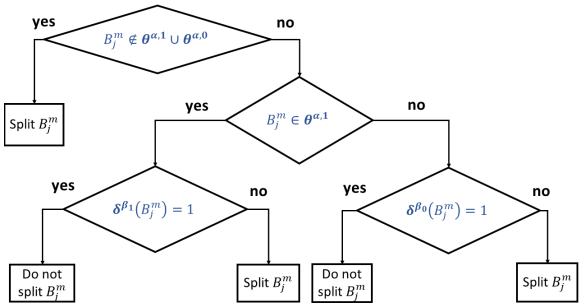


Figure 8: Diagram introducing the selection of the "best" wavelet packet base.

*f) Threshold of variations $\beta_1$:* Let $\beta_1$ be a real number in dB. For every non-attenuated sub-band $B_j^m \in \Theta^{\alpha,1}$, we associate a parameter $\delta^{\beta_1}(B_j^m) \in \{0,1\}$ defined as

$$\delta^{\beta_1}(B_j^m) = \begin{cases} 1 & \text{if } \max\limits_{f_k \in B_j^m} |H(f_k)|_{\text{dB}} - \min\limits_{f_k \in B_j^m} |H(f_k)|_{\text{dB}} \leq \beta_1 \\ 0 & \text{elsewhere} \end{cases}.$$

Same as the threshold $\beta_0$, when $\delta^{\beta_1}(B_j^m) = 1$, we can say that the channel $h$ does not vary significantly regarding to the threshold $\beta_1$ for the sub-band $B_j^m$.

It is useful to mention that the thresholds $\beta_0$ and $\beta_1$ can be compared to the difference $\min\limits_{f_k \in B_j^m} |H(f_k)| - \max\limits_{f_k \in B_j^m} |H(f_k)|$ instead of the ratio, or to the ratio $\frac{\min\limits_{f_k \in B_j^m} \text{SNR}(f_k)}{\max\limits_{f_k \in B_j^m} \text{SNR}(f_k)}$, or any other measure reflecting the selectivity of the channel.

### C. General assumptions

Adaptive techniques are only suitable for "duplex" communications between two stations, since the adaptive parameters need to be selected using a transmission in both directions, allowing channel estimation and signalization. In general, all adaptive techniques should consider the following items:

- Channel estimation and feedback to the receiver: the channel state information (CSI) is available through the estimation of the previous channel. The efficiency of the estimation is subject to low variations of the channel and its reciprocity. A reliable estimation of the channel should be sent to the transmitter because this latter needs to know the channel characteristics for the next transmission.
- Selection of the appropriate parameter for the next transmission: based on the available CSI, the transmitter selects the suitable adaptive parameter for the next transmission.
- Signalization of the employed parameter to the receiver: the selected adaptive parameter should be communicated or known by the receiver in order to properly demodulate the data.

### D. Selection of the best modulation

The scheme drawn in Fig. 7 provides an initial insight into the proposed adaptive modulation technique. Our target is to select a waveform that achieves a good PAPR/BER trade-off corresponding to a channel state. The selection of the best partition of the bandwidth goes through the following steps:

1) We assume that a perfect CSI of the channel $h$ is available at the transmitted side. The number $M$ of elementary frequencies as well as the set of thresholds $\alpha$, $\beta_0$ and $\beta_1$ are initially fixed.
2) The set of elementary frequencies $\{f_k\}_{k \in [\![0, M-1]\!]}$ is reviewed so as to decide whether each $f_k$ is attenuated or not by the channel fading according to the threshold $\alpha$. On this way, all the parameters $\theta^{\alpha}(f_k) \in \{0,1\}$ for each $f_k$ are updated.
3) Thereafter, the construction of the best basis is performed by evaluating the nodes from the root to the leaves along the tree branches, to decide whether to split or not the parent node $B_j^m$ into two children nodes $B_{j-1}^{2m}$ and $B_{j-1}^{2m+1}$. In order to make such a decision, the sub-band $B_j^m$ is evaluated according to the following criteria:
   - If $B_j^m \notin \Theta^{\alpha,1} \cup \Theta^{\alpha,0}$ ($B_j^m$ consists of a mixture of attenuated and non-attenuated frequencies) then the sub-band $B_j^m$ is splitted.
   - If $B_j^m \in \Theta^{\alpha,1}$ ($B_j^m$ is non-attenuated compared with the relevant threshold $\alpha$), then:
     - If $\delta^{\beta_1}(B_j^m) = 1$ (the variations of the channel in $B_j^m$ are significant regarding to the agreed threshold $\beta_1$) then the sub-band $B_j^m$ is splitted by two.
     - Otherwise, the sub-band $B_j^m$ is not splitted.
   - If $B_j^m \in \Theta^{\alpha,0}$ ($B_j^m$ is attenuated compared with $\alpha$), then
     - If $\delta^{\beta_0}(B_j^m) = 1$ (the variations of the channel in $B_j^m$ are significant regarding to $\beta_1$) then the sub-band $B_j^m$ is splitted.
     - Otherwise, the sub-band $B_j^m$ is not splitted.

The previous steps are briefly described in the diagram depicted in Fig. 8. By pruning the wavelet packet binary tree, we extract an admissible tree matching a specific division of the bandwidth. The resulting tree is related to a wavelet packet basis with which the data will be modulated and multiplexed.

### *E. Exchanging information between the transmitter and the receiver*

The quality of the channel estimation is relevant in the context of AWPM systems, because we require CSI to locate the attenuated frequencies, and define afterwards a suitable modulation basis for the channel. Generally, the receiver estimates the channel and a communication is established between the transmitter and the receiver so as to exchange CSI and/or adaptive parameters. Different ways of information exchange are possible. The choice of the appropriate approach takes into account, depending on the targeted application, spectral efficiency constraint, complexity and reliability. We provide below some examples of exchanging modes:

- The receiver performs channel estimation, extracts a channel measure and send it as a feedback to the transmitter.
  - If the extracted channel measure by the receiver represents the modulation base, then the transmitter uses the new modulation base at the next transmission. At the receiver side, the demodulation is properly performed since the receiver already knows the used modulation base.
  - If the extracted channel measure does not describe the modulation base, then we are exposed to two cases: either the transmitter will identify the modulation base and send its description to the receiver, or the receiver will also identify the modulation base and in that case the transmitter does not need to send this information.

The identification of the modulation base is performed in real time following the steps described in Section IV-D. Furthermore, it is conceivable to define beforehand, the modulation base for all the possible cases, and store the results in a database. The mapping is carried out from the pre-calculated database.

## V. Testing the AWPM algorithm for different threshold values

In this part, the AWPM modulation is applied for a specific channel. The objective is to emphasize the decomposition of the spectral bandwidth for different threshold values and evaluate the PAPR and BER performance of the resulting schemes.

AWPM is compared with OFDM ans SC-FDE to highlight that AWPM is an intermediate modulation between the two aforementioned waveforms, and also to support that the time-frequency of the modulated system affects the transmission performance. Moreover, AWPM is compared with the classical wavelet-based multi-carrier waveforms namely Wavelet-OFDM and WPM. The comparison is based on a discrete format approximation of Meyer wavelet named *Dmey*. This choice is justified by the good spectral properties of the Dmey wavelet. More details can be found in [28].

### *A. Example of a frequency selective fading channel*

Let $M = 64$ be the number of elementary frequencies and let $h$ be the impulse response of the channel given in Table I.

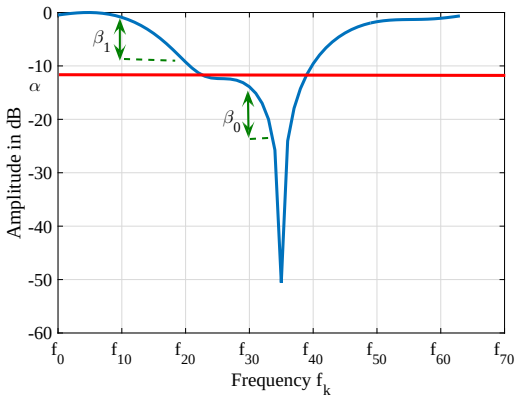


Figure 9: Frequency response $|H(f)|_{\text{dB}}$ of the channel $h$.

Fig. 9 describes the associated frequency response $|H(f_k)|_{\text{dB}}$, where $\{f_k\}_{k\in[\![0,M-1]\!]}$ is the set of the elementary frequencies. It can be easily observed that $h$ is a frequency selective fading channel. A deep spectral fading is identified around the frequency $f_{35}$, the coefficients of the channel around it are very low, and the noise will be very high while inverting the channel for equalization at the receiver.

### *B. Bandwidth partition using AWPM in a channel $h$*

Let $BW_{\text{total}} = M\Delta F = 64\Delta F$ be the total allocated bandwidth, such that $\Delta F$ is the width of the elementary sub-band $f_k$. The following set of thresholds is considered: $(\alpha = -10.45$ dB, $\beta_1 = +\infty$ dB, $\beta_0 = +\infty$ dB). The thresholds $\beta_1$ and $\beta_0$ are set to $+\infty$ dB for fostering the PAPR performance, since the sub-bands in this case are not divided according to the thresholds of variations but only according to the threshold of attenuations $\alpha$. In fact, the less we subdivide the bandwidth, the fewer sub-carriers overlap in time, the more we enhance the PAPR performance. However, the bandwidth should be subdivided in order to isolate the attenuated sub-bands from the non-attenuated ones in order to improve the BER performance. Hence the trade-off PAPR/BER. It is straightforward to notice that the frequencies $f_k$ such that $k \in [\![23, 40]\!]$ are affected by a deep fading regarding the threshold $\alpha$ ($|H(f_k)|_{\text{dB}} < \alpha$).

Let $x(t)$ be the resulting signal from the AWPM modulation, $x(t)$ can be expressed as:

$$x(t) = \sum_{n\in\mathbb{Z}} \sum_{m=0}^{M-1} a_m g_m(t - nT). \tag{12}$$

where $\{a_m\}$ are the input symbols and $\{g_m\}_{m\in[\![0,M-1]\!]}$ is the selected modulation basis. The channel bandwidth $BW_m$ occupied by every waveform $g_m$ from the modulation basis $\{g_m\}_{m\in[\![0,M-1]\!]}$ is expressed as follows:

$$BW_m = \begin{cases} 4\Delta F & \text{if } m \in [\![17, 20]\!] \\ 2\Delta F & \text{if } m \in [\![21, 24]\!] \\ 8\Delta F & \text{if } m \in [\![25, 48]\!] \\ 16\Delta F & \text{elsewhere} \end{cases}. \tag{13}$$

Table I: Coefficients of a frequency selective fading channel.

| $h_0$ | $h_1$ | $h_2$ | $h_3$ |
|---|---|---|---|
| $-0.3699 - i0.5782$ | $-0.4053 - i0.5750$ | $-0.0834 - i0.0406$ | $0.1587 - i0.0156$ |
| Delay = 0 | Delay = 1 | Delay = 2 | Delay = 3 |

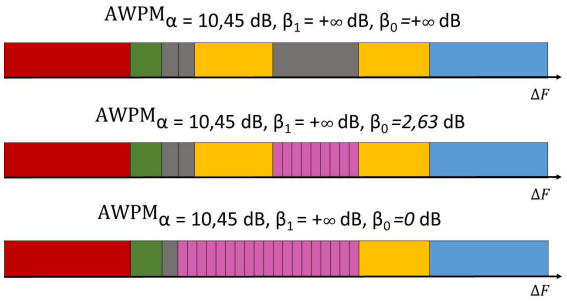


Figure 10: Distribution of the bandwidth associated to the channel $h$ in AWPM scheme for different threshold sets $(\alpha, \beta_1, \beta_0)$.

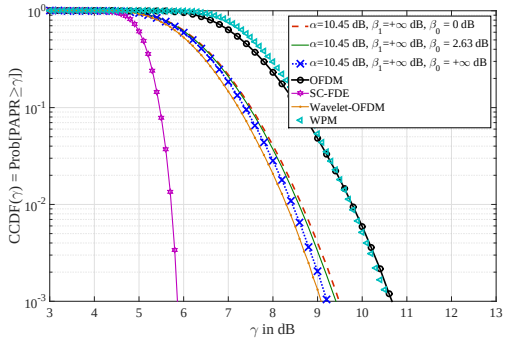


Figure 11: PAPR performance comparison for AWPM with threshold sets $(\alpha, \beta_1, \beta_0)$.

By assessing two other examples of a threshold set, we provide the associated sharing of the bandwidth:

- Example 2: $(\alpha = -10.45\,\text{dB}, \beta_1 = +\infty\,\text{dB}, \beta_0 = 2.63\,\text{dB})$:

$$BW_m = \begin{cases} 4\Delta F & \text{if } m \in [\![17, 20]\!] \\ 2\Delta F & \text{if } m \in [\![21, 24]\!] \\ 4\Delta F & \text{if } m \in [\![25, 32]\!] \\ \Delta F & \text{if } m \in [\![33, 40]\!] \\ 8\Delta F & \text{if } m \in [\![41, 48]\!] \\ 16\Delta F & \text{elsewhere} \end{cases}. \quad (14)$$

- Example 3: $(\alpha = -10.45\,\text{dB}, \beta_1 = +\infty\,\text{dB}, \beta_0 = 0\,\text{dB})$:

$$BW_m = \begin{cases} 4\Delta F & \text{if } m \in [\![17, 20]\!] \\ 2\Delta F & \text{if } m \in [\![21, 22]\!] \\ \Delta F & \text{if } m \in [\![23, 40]\!] \\ 8\Delta F & \text{if } m \in [\![41, 48]\!] \\ 16\Delta F & \text{elsewhere} \end{cases}. \quad (15)$$

The distribution of the bandwidth meeting the threshold sets $(\alpha = -10.45\,\text{dB}, \beta_1 = +\infty\,\text{dB}, \beta_0 = +\infty\,\text{dB})$, $(\alpha = -10.45\,\text{dB}, \beta_1 = +\infty\,\text{dB}, \beta_0 = 2.63\,\text{dB})$ and $(\alpha = -10.45\,\text{dB}, \beta_1 = +\infty\,\text{dB}, \beta_0 = 0\,\text{dB})$ can be illustrated in Fig. 10. Every setting of the threshold gives a different bandwidth partition, which corresponds to a different time-frequency characteristics of the resulting signal. We will see in the following section, that each setting provides different PAPR and BER performance.

### C. PAPR and BER performance for different thresholds

The PAPR and BER performances are assessed for different thresholds: $(\alpha = -10.45\,\text{dB}, \beta_1 = +\infty\,\text{dB}, \beta_0 = +\infty\,\text{dB})$, $(\alpha = -10.45\,\text{dB}, \beta_1 = +\infty\,\text{dB}, \beta_0 = 2.63\,\text{dB})$ and $(\alpha = -10.45\,\text{dB}, \beta_1 = +\infty\,\text{dB}, \beta_0 = 0\,\text{dB})$, whose the corresponding bandwidth decompositions are depicted in Fig. 10.

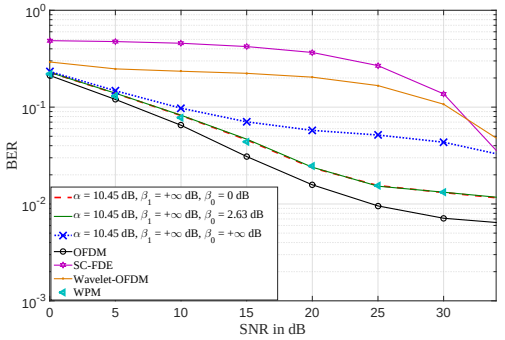


Figure 12: BER performance comparison for different threshold sets $(\alpha, \beta_1, \beta_0)$.

The simulations of all the schemes are implemented using the specific channel defined in Table I, with $M = 64$ sub-carriers, a 4-QAM constellation, and a zero forcing (ZF) equalization. The single carrier-frequency division equalization (SC-FDE) [29], [30] signal is filtered by a square root raised cosine (SRRC) filter of a roll-off factor equal to 0.2. A maximum number of decomposition equal to $J = \log_2(M)$ is used for the Wavelet-OFDM scheme, and WPM corresponds to a full decomposition of the bandwidth using the leaves of the wavelet binary tree.

Fig. 11 and Fig. 12 show that $\text{AWPM}_{\alpha=-10.45,\beta_1=+\infty,\beta_0=+\infty}$ scheme achieves the best PAPR performance and the weakest BER performance. Compared with $\text{AWPM}_{\alpha=-10.45,\beta_1=+\infty,\beta_0=2.63}$ and $\text{AWPM}_{\alpha=-10.45,\beta_1=+\infty,\beta_0=0}$, this scheme is the one that divides the least the bandwidth, enabling the non-overlapping of the sub-carriers (better PAPR), whereas not allowing to sufficiently isolate the attenuated frequencies into narrow sub-bands (worse BER). $\text{AWPM}_{\alpha=-10.45,\beta_1=+\infty,\beta_0=2.63}$ and $\text{AWPM}_{\alpha=-10.45,\beta_1=+\infty,\beta_0=0}$ schemes reach the best

Table II: Simulation parameters

| Parameters | Definition | Value |
|---|---|---|
| $M$ | Number of sub-carriers/ Number of elementary sub-bands | 128 |
| $S$ | Number of MCM symbols | 100 |
| SNR | Signal-to-noise ratio | $0:5:35$ |
| $n_{\text{iter}}$ | Number of frames | $10^6$ |
| $\Delta F$ | Inter-carrier spacing/ Width of elementary sub-bands | 15 kHz |
| $N$ | N-QAM Constellation | 4 or 16 |
| $\beta_1$ | Threshold on the non-attenuated frequencies | $+\infty$ dB |
| $\beta_0$ | Threshold on the attenuated frequencies | 0 dB |
| roll-off | Roll-off of the SRRC filter | 0.2 |

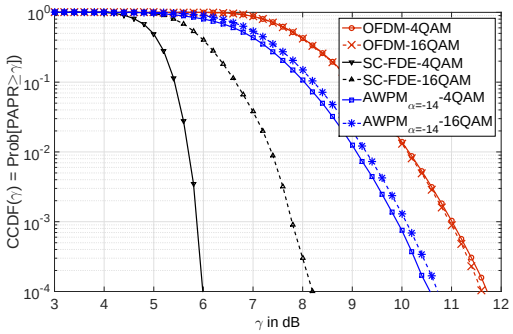


Figure 13: PAPR comparison for l'AWPM$_{\alpha=-14}$, OFDM and SC-FDE in ETU channel.

BER performance, with a slight gain in terms of PAPR for the former. A PAPR gain can be achieved (though insignificant in this example) while maintaining the same BER performance. OFDM and SC-FDE are features of the "extreme" cases of the bandwidth partition. SC-FDE is a single carrier modulation which does not split the bandwidth, while OFDM divides it entirely (Fig. 1). On one hand, SC-FDE, whose bandwidth decomposition can be comparable to AWPM$_{\alpha=-\infty,\beta_1=+\infty,\forall\beta_0}$, does not suffer from a large PAPR, but offers poor BER performance. On the other hand, OFDM, whose bandwidth decomposition is compared to AWPM$_{\alpha=0,\forall\beta_1,\beta_0=0}$, is experiencing a poor PAPR performance, while providing a valuable BER performance.

It is clear from the figures that the trade-off achieved by AWPM is far better from the ones realized by Wavelet-OFDM and WPM. For an almost equivalent PAPR performance, AWPM reaches better BER performance than Wavelet-OFDM. Similarly, for a quasi-identical BER performance, AWPM improves the PAPR performance compared with WPM (up to 1.2 dB for CCDF$= 10^{-3}$). Notice that, there is no need to completely split the bandwidth (WPM case), since we can achieve the same BER performance by subdividing the bandwidth only when necessarily while, consequently, improving the PAPR performance (AWPM case). Thus, AWPM outperforms the conventional wavelet-based waveforms.

Owing to its time-frequency properties, the AWPM system allows a reconfigurable modulation which can be adapted and adjusted to the targeted application and its performance criteria. The threshold selection is thus related to the desired outcomes in terms of PAPR and BER performance. For example, if the application has more constraints on the power consumption, the set of the thresholds should be chosen in a way to reduce the PAPR i.e ($\alpha, \beta_1, \beta_0$) tend to (-$\infty$ dB, $+\infty$ dB, $+\infty$ dB). Otherwise, the priority will be given to the BER ie ($\alpha, \beta_1, \beta_0$) tend to (0 dB, 0 dB, 0 dB).

## VI. Simulation results in ETU channel

In this section, the extended typical urban mode (ETU) [31] channel from LTE standard is used. The associated delays and gains are defined in Table III. The PAPR and BER performance are evaluated using the simulation parameters defined in Table II.

Since our target here is to evaluate the impact of the waveform on the PAPR and BER performance, coding techniques and PAPR reduction techniques are not used in these simulations. We assume a perfect channel estimation at the receiver side, and a feedback of CSI is sent to the transmitter. The channel is assumed to be stationary during this period. A cyclic prefix of $25\%$ is added to OFDM, AWPM and SC-FDE symbols. A ZF equalization is performed in the frequency domain for AWPM and SC-FDE receivers. The studied schemes are fairly compared in terms of the allocated bandwidth and the spectral efficiency.

### A. PAPR and BER performance

Fig. 13 depicts the PAPR performance of AWPM scheme for a threshold $\alpha = -14$ dB. Fig. 14 provides the associated BER performance. Both thresholds $\beta_0$ and $\beta_1$ are set to $+\infty$ in order to improve the PAPR. The simulation parameters are summarized in Table II.

AWPM$_{\alpha=-14}$ scheme reaches up to 1 dB gain in terms of PAPR (CCDF $= 10^{-3}$) for 16-QAM and 1.2 dB for 4-QAM compared with OFDM, with a loss of 2 dB for 16-QAM and 1.5 dB for 4-QAM in terms of SNR (BER$= 10^{-2}$). It is worth mentioning that the CCDF of OFDM does not change with the constellation, the impact of the "effective" number of sub-carriers on the CCDF "absorbs" the effect of the constellation. By contrast, the CCDF of SC-FDE varies substantially with the employed constellation. These variations are less pronounced for the AWPM scheme.

### B. Trade off: single carrier modulation and multi-carrier modulation

In this section, we emphasize on the trade-off PAPR/BER that offers the AWPM modulation, which can be viewed as a trade-off between single carrier modulation (e.g. SC-FDE) and classical multi-carrier modulation schemes (e.g. OFDM). The ETU channel (see Table III) is used in our simulations, and the threshold $\beta_0$ is set to 0 in order to well localize each attenuated frequency, and the threshold $\beta_1$ is set to $+\infty$ to combine the contiguous non-attenuated frequencies in the same sub-band.

Table III: Channel delay and power profile for ETU channel of LTE standard.

| Discrete delay ($ns$) | 0 | 50 | 120 | 200 | 230 | 500 | 1600 | 2300 | 5000 |
|---|---|---|---|---|---|---|---|---|---|
| Average path gains (dB) | -1.0 | –1.0 | -1.0 | 0.0 | 0.0 | 0.0 | -3.0 | -5.0 | -7.0 |

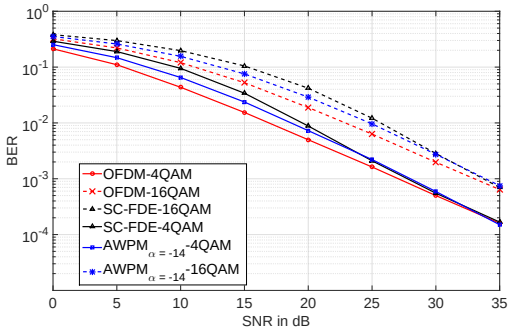


Figure 14: BER comparison for AWPM$_{\alpha=-14}$, OFDM and SC-FDE in ETU channel.

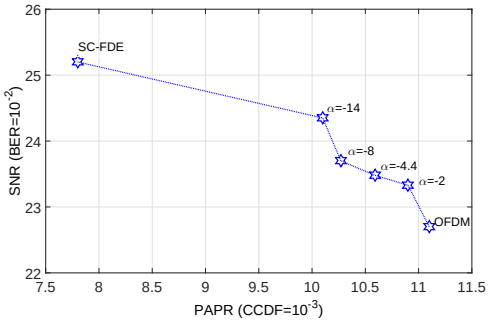


Figure 15: Trade-off PAPR/BER in ETU channel.

Fig. 15 presents the PAPR and SNR values for CCDF $= 10^{-3}$ and BER $= 10^{-2}$ achieved by SC-FDE, OFDM, and AWPM schemes for different thresholds $\alpha \in \{-14, -8, -4.4, -2\}$ dB. The 16-QAM constellation is applied in this comparison. We observe that the point (PAPR,SNR) for the different AWPM schemes lies between SC-FDE and OFDM, and reflects thus a trade-off between the good PAPR performance of SC-FDE and the good SNR performance of OFDM. We can assert once again, that AWPM is an intermediate scheme between the single carrier schemes and the classical multi-carrier schemes.

We remind that the choice of the threshold set $(\alpha, \beta_1, \beta_0)$ is very flexible and depends on the constraints of the intended application.

### *C. AWPM advantages over SC-FDE and OFDM*

Despite the positive PAPR performance achieved by SC-FDE modulation, it is not suitable for some adaptive techniques such as the power allocation per sub-carrier. Moreover, if the CSI is available at the receiver side, we can "avoid" transmitting useful data in the attenuated sub-carriers for a multi-carrier system. However, the employment of these techniques is not compatible with SC-FDE structure.

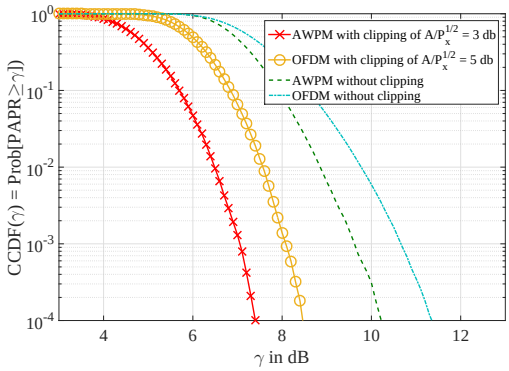


Figure 16: PAPR comparison for AWPM and OFDM using clipping and filtering. The clipping level A is set to get a similar BER performance.

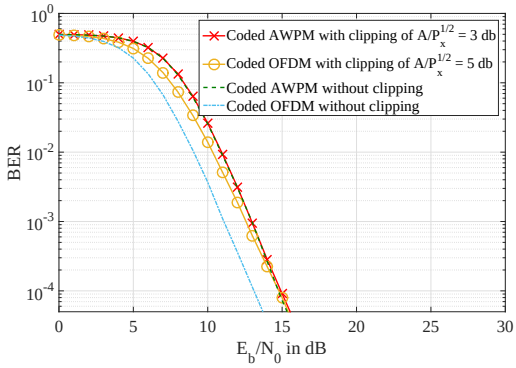


Figure 17: BER comparison for coded AWPM and coded OFDM using clipping and filtering for PAPR reduction.

Compared with OFDM, AWPM modulation enables a better PAPR by choosing an appropriate partition of the channel bandwidth. The flexibility of the bandwidth decomposition gives to AWPM the opportunity to use some adaptation techniques in a more flexible way. In particular, an adaptation over sub-bands with different widths can be applied to adaptive modulation and coding (AMC) techniques [32]. Furthermore, AWPM offers a large choice of wavelet families.

Finally, we can conclude that the AWPM system can contribute to overcome certain limitations of the single carrier modulation, while satisfying several advantages of classical multi-carrier modulation, and allowing other adaptation possibilities which are not compatible with the commonly used modulations.

### *D. Comparison of coded systems using a PAPR reduction technique*

In real systems, OFDM is equipped with a PAPR reduction technique in order to avoid power amplifier saturation. Clip-

ping is one of the most used and less complex PAPR reduction techniques, which is backward compatible and does not reduce the data rate of the transmission. Clipping method is usually followed by a filtering to reduce the non-linear distortions caused by the clipping operation. The major drawback of clipping is the increased BER due to the generated inter-carrier interference. Thus, a PAPR improvement is traded against BER performance. Moreover, OFDM is always deployed with channel coding to improve its resilience to frequency selective channels, which also contributes in the aforementioned PAPR/BER trade-off.

In this section, AWPM and OFDM are compared using clipping as a PAPR reduction technique along with a conventional coding with a Viterbi detection. A filtering is applied after clipping. A Rayleigh channel is considered, where its impulse response coefficients $h = (h(1), h(2) \dots h(\nu))$ are supposed to be circularly symmetric complex Gaussian random variables with $\mathcal{CN}(0, \frac{1}{\nu})$ distribution. The following setting are fixed for the simulations in this section: $M = 64$, $N = 4$, $\nu = 4$, code rate$= \frac{1}{2}$, $(\alpha, \beta_1, \beta_0)$ = (14 dB, $+\infty$ dB, 0 dB), $A$ is the clipping level, and $P_x$ is the power of the transmitted signal before clipping.

Fig. 16 depicts the PAPR performance of AWPM and OFDM using clipping and filtering in order to reduce the PAPR, and Fig. 17 provides the associated BER performance for coded systems. Clipping function is performed in the time domain, and filtering takes place in the frequency domain. The PAPR and BER performance are averaged over the different realizations of the Rayleigh channel. In order to fairly compare the PAPR/BER trade-off, we have identified the clipping levels that give similar BER performance for both AWPM and OFDM, and then we have evaluated the associated PAPR performance. AWPM unsurprisingly outperforms OFDM in terms of PAPR (1 dB gain). AWPM and OFDM show a fairly close BER performance, although a slight improvement is observed for OFDM for low SNR values. We can also notice from Fig. 17 that the distortions introduced by clipping deteriorates the BER performance of OFDM. The impact of clipping is less significant for AWPM which can be explained by the consideration that high peak powers are less likely to happen in AWPM than in OFDM. From these observations, we can conclude that, even when combined with clipping and filtering, AWPM achieves a better PAPR/BER trade-off than OFDM.

## VII. Conclusions

The proposed scheme in this paper is a flexible modulation that adapts the wavelet packet based waveform to the channel properties. The flexibility of the time-frequency tiling of the wavelet packet transform allows the AWPM scheme to spread non-uniformly the channel bandwidth in order to adapt it to the frequency selectivity of the communication channel. We have proposed an adaptive technique for AWPM scheme, based on a set of thresholds $(\alpha, \beta_1, \beta_0)$. The threshold $\alpha$ enables to select the attenuated frequencies in a fading environment, while the threshold $\beta_1$ ($\beta_0$ resp.) allows to gather in the same sub-band the attenuated (non-attenuated resp.) contiguous frequencies non-affected by the channel variations. In order to select the "best" partition of the bandwidth, and identify the "best" modulation base, we have described an adaptive algorithm through various steps. We have evaluated the performance of the AWPM modulation in frequency selective channel and compared it with several waveforms from the literature: OFDM, SC-FDE, Wavelet-OFDM, and WPM. Channel coding and clipping have also been considered in our comparisons. Our conclusions show that the proposed AWPM scheme provides good achievement in terms of PAPR/BER trade-off.

AWPM is a new proposed scheme that provides a new conception of adapting the bandwidth partition to the channel characteristics. As any new system, it needs more investigations to evaluate its performance, including inter-carrier interference analysis, imperfect knowledge of the channel state information, channel equalization methods, and study of the complexity, which will be addressed in further works.

## References


[1] S. Sesia, I. Toufik, and M. Baker, *LTE-the UMTS Long Term Evolution*. Wiley Online Library, 2015.

[2] S. Kaiser, "OFDM Code-Division Multiplexing in Fading Channels," *IEEE Transactions on Communications*, vol. 50, no. 8, pp. 1266–1273, 2002.

[3] M. Chafii, J. Palicot, R. Gribonval, and F. Bader, "A Necessary Condition for Waveforms with Better PAPR than OFDM," *IEEE Transactions on Communications*, vol. PP, no. 99, pp. 1–1, 2016.

[4] H. Bogucka and A. Conti, "Degrees of freedom for energy savings in practical adaptive wireless systems," *Communications Magazine, IEEE*, vol. 49, no. 6, pp. 38–45, 2011.

[5] J. Palicot and Y. Louët, "Power ratio definitions and analysis in single carrier modulations," in *EUSIPCO, 2005*. IEEE, 2005, pp. 1–4.

[6] R. W. Bäuml, R. F. Fischer, and J. B. Huber, "Reducing the peak-to-average power ratio of multicarrier modulation by selected mapping," *Electronics Letters*, vol. 32, no. 22, pp. 2056–2057, 1996.

[7] Y. Louët, "Etudes et performances des codes de Reed-Muller pour la réduction du facteur de crête dans les modulations OFDM," *These de Doctorat, Université de Rennes I*, 2000.

[8] J. Tellado-Mourelo, "Peak to average power reduction for multicarrier modulation," Ph.D. dissertation, Stanford University, 1999.

[9] D. Guel and J. Palicot, "Clipping formulated as an adding signal technique for ofdm peak power reduction," in *Vehicular Technology Conference, 2009. VTC Spring 2009. IEEE 69th*. IEEE, 2009, pp. 1–5.

[10] I. Kalet, "The Multitone Channel," *Communications, IEEE Transactions on*, vol. 37, no. 2, pp. 119–124, 1989.

[11] P. S. Chow, J. M. Cioffi, J. Bingham *et al.*, "A practical discrete multitone transceiver loading algorithm for data transmission over spectrally shaped channels," *IEEE Transactions on communications*, vol. 43, no. 234, pp. 773–775, 1995.

[12] A. Czylwik, "Adaptive OFDM for Wideband Radio Channels," in *Global Telecommunications Conference, 1996. GLOBECOM '96. 'Communications: The Key to Global Prosperity*, vol. 1, Nov 1996, pp. 713–718 vol.1.

[13] S. Mallat, *A Wavelet Tour of Signal Processing*. Academic press, 2008.

[14] R. Zakaria and D. L. Ruyet, "A Novel Filter-Bank Multicarrier Scheme to Mitigate the Intrinsic Interference: Application to MIMO Systems," *IEEE Transactions on Wireless Communications*, vol. 11, no. 3, pp. 1112–1123, March 2012.

[15] B. Borna and T. N. Davidson, "Efficient Design of FMT Systems," *IEEE transactions on communications*, vol. 54, no. 5, pp. 794–797, 2006.

[16] W. Kozek and A. F. Molisch, "Nonorthogonal pulseshapes for multicarrier communications in doubly dispersive channels," *Selected Areas in Communications, IEEE Journal on*, vol. 16, no. 8, pp. 1579–1589, 1998.

[17] N. Michailow, M. Matthé, I. S. Gaspar, A. N. Caldevilla, L. L. Mendes, A. Festag, and G. Fettweis, "Generalized Frequency Division Multiplexing for 5th Generation Cellular Networks," *IEEE Transactions on Communications*, vol. 62, no. 9, pp. 3045–3061, 2014.

[18] V. Vakilian, T. Wild, F. Schaich, S. ten Brink, and J.-F. Frigon, "Universal-filtered multi-carrier technique for wireless systems beyond LTE," in *2013 IEEE Globecom Workshops (GC Wkshps)*. IEEE, 2013, pp. 223–228.
[19] S. Galli and O. Logvinov, "Recent Developments in the Standardization of Power Line Communications within the IEEE," *Communications Magazine, IEEE*, vol. 46, no. 7, pp. 64–71, 2008.
[20] M. Chafii, J. Palicot, and R. Gribonval, "The Wavelet Modulation: an Alternative Modulation with Low Energy Consumption," *Special Issue Energy in Radiosciences, "Compte Rendus de l'Académie des Sciences (CRAS)"*, 2017.
[21] S. L. Linfoot, M. K. Ibrahim, and M. M. Al-Akaidi, "Orthogonal Wavelet Division Multiplex: An Alternative to OFDM," *Consumer Electronics, IEEE Transactions on*, vol. 53, no. 2, pp. 278–284, 2007.
[22] A. Lindsey, "Wavelet packet modulation for orthogonally multiplexed communication," *Signal Processing, IEEE Transactions on*, vol. 45, pp. 1336–1339, May 1997.
[23] K. M. Wong, J. Wu, T. N. Davidson, Q. Jin, and P.-C. Ching, "Performance of Wavelet Packet-Division Multiplexing in Impulsive and Gaussian Noise," *IEEE Transactions on Communications*, vol. 48, no. 7, pp. 1083–1086, 2000.
[24] M. Gautier, C. Lereau, M. Arndt, and J. Lienard, "PAPR analysis in wavelet packet modulation," in *Communications, Control and Signal Processing, 2008. ISCCSP 2008. 3rd International Symposium on*. IEEE, 2008, pp. 799–803.
[25] H. Nikookar, *Wavelet Radio: Adaptive and Reconfigurable Wireless Systems Based on Wavelets*. Cambridge University Press, 2013.
[26] R. R. Coifman, Y. Meyer, and V. Wickerhauser, "Wavelet analysis and signal processing," in *In Wavelets and their Applications*. Citeseer, 1992.
[27] M. Vetterli and J. Kovačević, "Wavelets and subband coding," 2007.
[28] M. Chafii, J. Palicot, R. Gribonval, and A. Burr, "Power Spectral Density Limitations of the Wavelet-OFDM System," *Eusipco, Budapest, Hungary*, 2016.
[29] D. Falconer, S. L. Ariyavisitakul, A. Benyamin-Seeyar, and B. Eidson, "Frequency Domain Equalization for Single-Carrier Broadband Wireless Systems," *IEEE Communications Magazine*, vol. 40, no. 4, pp. 58–66, 2002.
[30] F. Pancaldi, G. M. Vitetta, R. Kalbasi, N. Al-Dhahir, M. Uysal, and H. Mheidat, "Single-Carrier Frequency Domain Equalization," *IEEE Signal Processing Magazine*, vol. 25, no. 5, pp. 37–56, September 2008.
[31] T. ETSI, "136 101 V8. 23.0 (3GPP TS 36.101 V8. 23.0 Release 8)."
[32] K.-B. Song, A. Ekbal, S. T. Chung, and J. M. Cioffi, "Adaptive Modulation and Coding (AMC) for Bit-Interleaved Coded OFDM (BIC-OFDM)," *IEEE Transactions on Wireless Communications*, vol. 5, no. 7, pp. 1685–1694, 2006.

**Marwa Chafii** (M'13) is currently a research group leader at Vodafone Chair Mobile Communications Systems, TU Dresden, Germany. She received her Ph.D. degree in Telecommunications from CentraleSupélec, (Rennes, France) in 2016. Her research interests include advanced waveforms for multi-carrier systems, the peak-to-average power ratio (PAPR) reduction problem, cellular Internet of Things (C-IoT) and Cognitive Radio. She received in 2013, her research master's degree in the field of advanced wireless communication systems (SAR) from CentraleSupélec (Paris, France), and her engineering diploma in telecommunications from Institut National des Postes et Télécommunications (INPT) in Morocco. Between 2014 and 2016, she has been visiting, for short scientific research missions, Poznan University of Technology (Poland), University of York (UK), Yokohama National University (Japan), and University of Oxford (UK).

**Jacques Palicot** received, in 1983, his PhD degree in Signal Processing from the University of Rennes. Since 1988, he has been involved in studies about equalization techniques applied to digital transmissions and analog TV systems. Since 1991 he has been involved mainly in studies concerning the digital communications area and automatic measurements techniques. He has taken an active part in various international bodies EBU, CCIR, URSI, and within RACE, ACTS and IST European projects. He has published various scientific articles notably on equalization techniques, echo cancellation, hierarchical modulations and Software Radio techniques. He is author or co-author of more than 300 publications with more than 50 in journals, two books and 22 patents. He is currently involved in adaptive Signal Processing, digital communications, Software Radio, Cognitive radio and Green Radio. From November 2001 to September 2003 he had a temporary position with INRIA/IRISA in Rennes. He serves as Associate Editor for EURASIP JASP since 2008. He also served as lead guest editor for several Special Issues on Software Radio, Cognitive Radio and Green Radio. He was Co General Chairman of ISCIT 2011, Co General Chairman of Next-GWiN 2014, Technical Program Chairman of CROWNCOM 2009, Technical Program Chairman of GREENCOM 2013 and Technical Program Chairman of CRN Symposium of ICC 2014. Since October 2003 he is with CentraleSupélec in Rennes where he leads the Signal Communications and Embedded Electronics (SCEE) research team.

**Rémi Gribonval** (M'02,SM'08,FM'14) is a Senior Researcher with Inria (Rennes, France), and the scientific leader of the PANAMA research group on sparse audio processing. A former student at École Normale Supérieure (Paris, France), he received the Ph. D. degree in applied mathematics from Université de Paris-IX Dauphine (Paris, France) in 1999, and his Habilitation à Diriger des Recherches in applied mathematics from Université de Rennes I (Rennes, France) in 2007. His research focuses on mathematical signal processing, machine learning, approximation theory and statistics, with an emphasis on sparse approximation, audio source separation and compressed sensing. He founded the series of international workshops SPARS on Signal Processing with Adaptive/Sparse Representations. In 2011, he was awarded the Blaise Pascal Award in Applied Mathematics and Scientific Engineering from the SMAI by the French National Academy of Sciences, and a starting investigator grant from the European Research Council.

**Faouzi Bader** (SM'07) received his PhD degree (with Honours) in Telecommunications in 2002 from Universidad Politécnica de Madrid (UPM), Madrid-Spain. He joined the Centre Technologic de Telecomunicacions de Catalunya (CTTC) in Barcelona-Spain as Associate researcher in 2002, and nominated in 2006 Senior Research Associate at same institution. Since June 2013, he is as Associate Professor at CentraleSupélec in Rennes- France. His research activities mainly focus on advanced multi-carrier waveforms (OFDM(A), (non-) uniform multimode filter based multicarrier schemes) and frequency allocation techniques in relay cognitive environment. He has been involved in several European projects from the 5th-7th EC research frameworks, and from 2012-2013 he was nominated general coordinator and manager of the EC funded research project ICT "EMPhAtiC" focusing on "Enhanced Multicarrier Techniques for Professional Ad-Hoc and Cell-Based Communications". He has published over 120 papers in peer-reviewed journals and international conferences, more than 13 book chapters, and published 3 books. He served as Technical Program Committee member in major IEEE ComSoc and VTS conferences, and as the general chair of the eleventh edition of the ISWCS'2014 conference, and the co-chair of the ISWCS 2015 edition. He is IEEE Senior Member from 2007.